Evaluating the potential for a direct marine source of NO_x to the atmosphere within GEOS-Chem

Matthew L. Loman[1], Lee T. Murray[1], Thomas S. Weber[1], Viral Shah[2] [1]University of Rochester, Rochester, NY, USA [2]Harvard University, Cambridge, MA, USA

NASA ATom Campaign

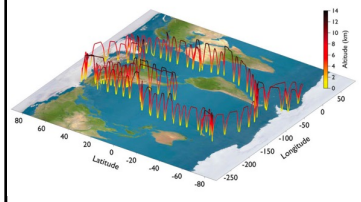

Figure 1: Flight path of the third ATom deployment to illustrate the vertical sampling strategy used in this mission. NASA's DC-8 aircraft flew at 0.2-12 km altitude over the Pacific, Southern, and Atlantic Oceans as well as the Arctic.

- NASA Atmospheric Tomography (ATom) mission: four flights 2016-2018, one in each season, following a common flight path (**Figure 1**)
- These observations allow us to evaluate the reactive nitrogen budget of the remote atmosphere in a global chemical transport model for the first time
- Initial model results (**Figure 2**) showed consistent low bias in the marine boundary layer
- Here, we have tested the hypothesis that this low bias can be explained by a marine source of NO to the atmosphere
- However, further simulations in GEOS-Chem 13.1.1 could not reproduce the bias shown in **Figure 2**.

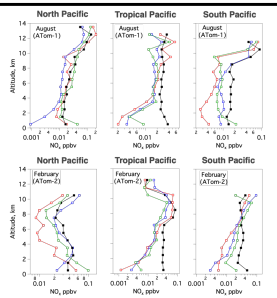

Figure 2: Initial model results plotted by Chelsea Thompson. Red: GEOS-Chem; green: CAM-Chem; blue: GMI; black: ATom observations.

Nitrite Photolysis

Location	Emission flux (kg N km^{-2} a^{-1})	Reference
Central equatorial Pacific[a]	2.1	*Zafiriou & McFarland* (1981)
Seto Inland Sea	3.4	*Olasehinde et al.* (2010)
Yellow Sea & Bohai Sea	4.3	*Tian et al.* (2019)
Western tropical North Pacific Ocean[b]	12.3	*Tian et al.* (2020)

[a]Approximately -2.5°S to 2.5°N, 180 to 80°W. [b]2 to 36°N, 143 to 146°E.

Table 1: Published estimates of NO emissions attributed to nitrite photolysis. Attempts to measure emission or dissolved concentration of marine NO have been limited to regional studies.

$$NO^-_{2(aq)} + h\nu \rightarrow NO_{(g)} + O^-_{(aq)} \quad (295 \leq \lambda \leq 410\ \text{nm}) \qquad \textbf{(R1)}$$

- Nitrite ion dissolved in the ocean can photolyze to produce NO (**R1**), supersaturating the surface ocean by a factor of up to 10^4
- Box model studies indicate that nitrite photolysis is necessary to reproduce observed ozone mixing ratios in the marine boundary layer (*Ayers et al.*, 1997; *Thompson and Lenschow*, 1984)
- Has not been included in models due to presumed small magnitude and distance from population centers and measurement networks.

Marine NO Simulation

$$[NO]_{(aq)} = \beta\, J_{NO_2}\, [NO^-_2]_{(aq)}\, \Delta t \qquad \textbf{(E1)}$$

- We run GEOS-Chem 13.1.1 at 4º x 5º resolution with 47 vertical layers from July 2016 – July 2018 to cover ATom campaign dates
- There are no global measurements of dissolved NO, so we use dissolved nitrite concentration as model input (**Figure 3**) and parameterize photolysis (**E1**)
- **E1**: $J_{NO^-_2} \approx J_{NO_2}$ multiplied by seawater attenuation factor β that represents attenuation of light in water. Δt is model emissions timestep
- β determined by first running the model with β = 1, then estimated as ratio of median NOx bias in original model to median NOx bias in β = 1 simulation. Results are shown in **Table 2**.

Latitude band	β
Arctic (60°–90°N)	0.00130
Northern Midlatitudes (23°–60°N)	0
Tropics (23°S–23°N)	0.00641
Southern Midlatitudes (50°–23°S)	0.00025
Southern Ocean (90°–50°S)	0.00013

Table 2: Values of β calculated as described above. β is determined separately for different latitude bands.

- Marine NO emissions add up to 10 pptv NOx (up to 15 pptv NO_y; up to 20 pptv O3) to the remote marine boundary layer, with a maximum in the tropical Pacific. Vertical profiles are shown in **Fig. 5b**.
- Relative increases (500% in NOx; 100% in NO_y; 15% in O3) are greatest over the Southern Ocean.
- Possible future directions:
  - Improvement in photolysis parameterization to account for differences in quantum yield between nitrite and NO2
  - Application of observational constraints on β
  - Calculating separate values for β by ocean basin
  - Statistical mapping of dissolved nitrite concentration based on relationships with chlorophyll and dissolved nitrate

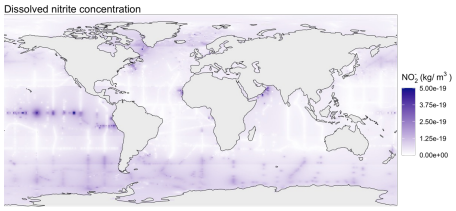

Figure 3: Inverse distance weighted interpolation of observed dissolved nitrite ion in the top 5m of the ocean from GLODAPv2.2020.

Emissions (Tg N a^{-1})	Atlantic	Indian	Pacific	Global	Total NO_y
Arctic (60° - 90°N)	0.0046	-	0.0004	0.0050	0.7959
Northern Midlatitudes (23° - 60°N)	0.0289	-	0.0360	0.0649	27.3262
Tropics (23°S - 23°N)	0.0361	0.0500	0.1967	0.2828	22.0001
Southern Midlatitudes (50° - 23°S)	0.0464	0.0515	0.0772	0.1751	3.1770
Antarctic (90° - 50°S)	0.0150	0.0165	0.0310	0.0625	0.0881
Total	**0.1310**	**0.1180**	**0.3413**	**0.5903**	**53.3873**

Table 3: Two year mean of simulated oceanic NOx emissions separated by ocean basins as shown in **Figure 4**. Global budget of NOx from the simulation is included for comparison.

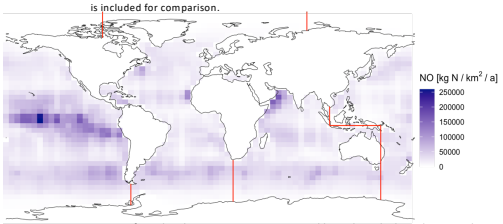

Figure 4: Two year mean of simulated oceanic NOx emissions. Red lines show the boundaries used to separate ocean basins in **Table 3**.

Reactive Nitrogen in GEOS-Chem

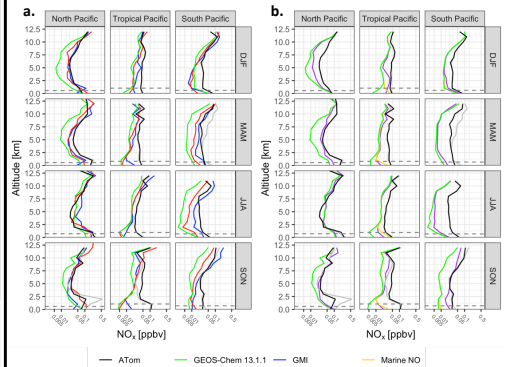

Figure 5: Vertical profiles of median NOx mixing ratio in various simulations. **Fig. 5a** reproduces **Fig. 2** alongside GEOS-Chem 13.1.1 output and both preliminary (used in **Fig. 2**) and finalized ATom observations for comparison; **Fig. 5b** shows GEOS-Chem 13.1.1 simulations edited to include marine NO and nitrate photolysis as additional sources of NOx. Boundary layer height is shown with a dotted gray line.

- **Figure 5** shows the effects of both model version and additional emissions on vertical profiles of NOx over the Pacific Ocean in GEOS-Chem.
- Recent work by Viral Shah et al. (in prep) indicates that inclusion of photolysis of nitrate aerosol particles to NOx in GEOS-Chem 12.9 improves the model's ability to reproduce concentrations of NOx over the ocean observed in the ATom mission. This work is reproduced in GEOS-Chem 13.1.1 in **Fig. 5b.**

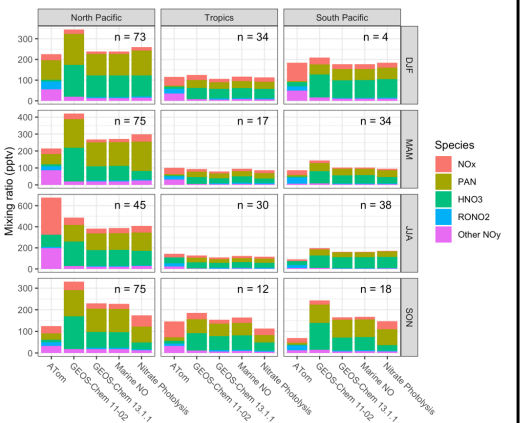

Figure 6: Marine boundary layer NO_y partitioning observed in ATom campaigns compared to simulations in GEOS-Chem, separated by season and latitude bin. At the top right of each subplot is the number of ATom observations used. In GEOS-Chem simulations, 'Other NO_y' = NO_3 + HNO_2 + HNO_4 + 2*N_2O_5 + $BrNO_2$ + $BrNO_3$ + $ClNO_2$ + $ClNO_3$ + INO + $IONO_2$ + 0.1*(NIT + NITs).

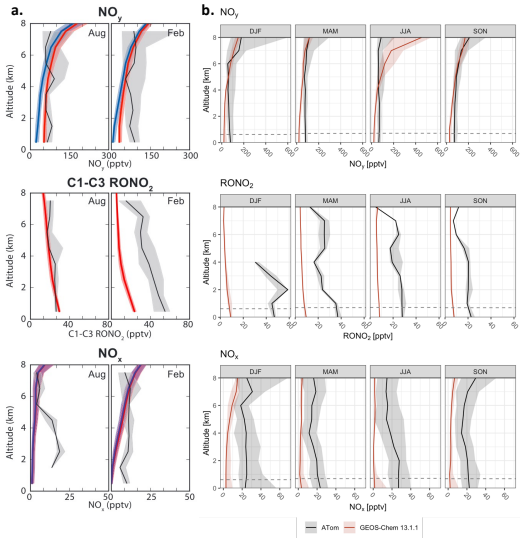

Figure 7: (**a**) Vertical profiles over the Southern Ocean reproduced from Fisher et al. (2018), in which alkyl nitrate emissions from the ocean were simulated in GEOS-Chem for the first time. Blue = GEOS-Chem 9-02; red = GEOS-Chem 9-02 with alkyl nitrate emissions; black = ATom observations. (**b**) The same plots as (a) in GEOS-Chem 13.1.1 with finalized ATom observations. Boundary layer height is shown with a dotted gray line.

- **Figure 6** compares the observed NO_y budget with various GEOS-Chem simulations.
- The number of ATom observations in each subplot is limited by alkyl nitrate (RONO2) which was measured only in flask samples during the ATom campaign. About 160 flasks were collected per flight.
- Submicron nitrate aerosol particles (about 10%) included as 'Other NO_y' for GEOS-Chem bars. These particles are likely included in ATom NO_y measurements (Chelsea Thompson, personal communication, Nov. 2021)
- Although GEOS-Chem 13.1.1 performs more poorly than 11-02 in NOx mixing ratios, total NO_y mixing ratios are closer to observed values.
- The addition of nitrate aerosol photolysis to GEOS-Chem 13.1.1 improves simulated HNO_3 mixing ratio.
- **Figure 7** compares vertical profiles of NO_y, alkyl nitrates, and NOx over the Southern Ocean (50º to 70º S) between Fisher et al. (2018) and GEOS-Chem 13.1.1.
- **Fig. 7a** uses preliminary ATom data (not shown in **Fig. 7b**), accounting for the
- We are unable to reproduce the vertical profiles of alkyl nitrate seen in **Fig. 7a**. Boundary layer mixing ratio of alkyl nitrates reach a maximum of around 10 pptv, compared to around 30 pptv in GEOS-Chem 9-02.
- There has been a significant change in the way GEOS-Chem simulates reactive nitrogen. Based on the changes in mixing ratios of alkyl nitrates, which do not have another source in GEOS-Chem and have not to our knowledge experienced major changes since their implementation, this is likely due to changes in GEOS-Chem's chemical mechanism.

References

Adesina, A. O., & Sakugawa, H. (2021, AUG 10). Photochemically generated nitric oxide in seawater: The peroxynitrite sink and its implications for daytime air quality. Science of the Total Environment, 781 . doi: 10.1016/j.scitotenv.2021.146683

Ayers, G., Granek, H., & Boers, R. (1997, JUN). Ozone in the marine boundary layer at Cape Grim: Model simulation. JOURNAL OF ATMOSPHERIC CHEMISTRY , 27 (2), 179-195. doi: 10.1023/A:1005828930552

Barletta, B., Biggs, B., Blake, D., Blake, N., Hoffman, A., Hughes, S., ... Woods, C. (2019). Atom: L2 halocarbons and hydrocarbons from the UC Irvine whole air sampler (WAS). ORNL Distributed Active Archive Center. doi: 10.3334/ORNLDAAC/1751

Burkholder, J. B., Sander, S. P., Abbatt, J., Barker, J. R., Cappa, C., Crounse, J. D., ... Wine, P. H. (2019). Chemical Kinetics and Photochemical Data for Use in Atmospheric Studies, Evaluation No. 19 (JPL Publication No. 19-5). Pasadena, California: Jet Propulsion Laboratory. Retrieved from http://jpldataeval.jpl.nasa.gov/

Fisher, J. A., Atlas, E. L., Barletta, B., Meinardi, S., Blake, D. R., Thompson, C. R., ... Murray, L. T. (2018). Methyl, Ethyl, and Propyl Nitrates: Global Distribution and Impacts on Reactive Nitrogen in Remote Marine Environments. Journal of Geophysical Research: Atmospheres, 123 (21), 12,429-12,451. doi: 10.1029/2018JD029046

Flocke, F., Weinheimer, A., Swanson, A., Roberts, J., Schmitt, R., & Shertz, S. (2005, SEP). On the measurement of pans by gas chromatography and electron capture detection. JOURNAL OF ATMOSPHERIC CHEMISTRY, 52 (1), 19-43. doi: 10.1007/s10874-005-6772-0

Key, R., Olsen, A., van Heuven, S., Lauvset, S. K., Velo, A., Lin, X., ... Suzuki, T. (2015). Global Ocean Data Analysis Project, Version 2 (GLODAPv2) (ORNL/CDIAC-162 No. NDP-093). Oak Ridge, Tennessee: Carbon Dioxide Information Analysis Center, Oak Ridge National Laboratory, US Department of Energy. doi: 10.3334/CDIAC/OTG.NDP093 GLODAPv2

Liu, C.-Y., Feng, W.-H., Tian, Y., Yang, G.-P., Li, P.-F., & Bange, H. W. (2017). Determination of dissolved nitric oxide in coastal waters of the Yellow Sea off Qingdao. Ocean Science, 13 (4), 623–632. doi: 10.5194/os-13-623-2017

Olasehinde, E. F., Takeda, K., & Sakugawa, H. (2010). Photochemical production and consumption mechanisms of nitric oxide in seawater. Environmental Science & Technology, 44 (22), 8403-8408. doi: 10.1021/es101426x

Olsen, A., Key, R. M., van Heuven, S., Lauvset, S. K., Velo, A., Lin, X., ... Suzuki, T. (2016). The Global Ocean Data Analysis Project version 2 (GLODAPv2) - an internally consistent data product for the world ocean. Earth System Science Data, 8 (2), 297–323. doi: 10.5194/essd-8-297-2016

Thompson, A. M., & Lenschow, D. H. (1984). Mean profiles of trace reactive species in the unpolluted marine surface layer. Journal of Geophysical Research: Atmospheres, 89 (D3), 4788-4796. doi: 10.1029/JD089iD03p04788

Thompson, C. R., Wofsy, S. C., Prather, M. J., Newman, P. A., Hanisco, T. F., Ryerson, T. B., ... Zeng, L. (2021). THE NASA ATMOSPHERIC TOMOGRAPHY (ATom) MISSION: Imaging the Chemistry of the Global Atmosphere. Bulletin of the American Meteorological Society, 1 - 53. doi: 10.1175/BAMS-D-20-0315.1

Tian, Y., Xue, C., Liu, C.-Y., Yang, G.-P., Li, P.-F., Feng, W.-H., & Bange, H. W. (2019). Nitric oxide (NO) in the Bohai Sea and the Yellow Sea. Biogeosciences, 16 (22), 4485–4496. doi: 10.5194/bg-16-4485-2019

Tian, Y., Yang, G.-P., Liu, C.-Y., Li, P.-F., Chen, H.-T., & Bange, H. W. (2020). Photoproduction of nitric oxide in seawater. Ocean Science, 16 (1), 135–148. doi: 10.5194/os-16-135-2020

Treinin, A., & Hayon, E. (1970). Absorption spectra and reaction kinetics of NO2, N2O3, and N2O4 in aqueous solution. Journal of the American Chemical Society, 92 (20), 5821-5828. doi: 10.1021/ja00723a001

Wall, S. M., John, W., & Ondo, J. L. (1988). Measurement of aerosol size distributions for nitrate and major ionic species. Atmospheric Environment (1967), 22 (8), 1649-1656. doi: 10.1016/0004-6981(88)90392-7

Ye, C., Zhang, N., Gao, H., & Zhou, X. (2017). Photolysis of Particulate Nitrate as a Source of HONO and NOx. Environmental Science & Technology, 51 (12), 6849-6856. doi: 10.1021/acs.est.7b00387

Zafiriou, O. C., & McFarland, M. (1981). Nitric oxide from nitrite photolysis in the central equatorial Pacific. Journal of Geophysical Research: Oceans, 86 (C4), 3173-3182. doi: 10.1029/JC086iC04p03173

Zafiriou, O. C., McFarland, M., & Bromund, R. H. (1980). Nitric oxide in seawater. Science, 207 (4431), 637-639. doi: 10.1126/science.207.4431.637

Summary and Acknowledgements

- GEOS-Chem 13.1.1 simulated NOx mixing ratios are biased low in the remote atmosphere, and 13.1.1 performs worse than 11-02 in the free troposphere.
- Simulations of total reactive nitrogen are still biased high in HNO_3 and PAN, but alkyl nitrates and NOx in 13.1.1 perform worse than in previous versions of GEOS-Chem.
- Additional sources of NOx to the remote atmosphere via marine emission or photolysis of nitrate aerosol particles push simulated mixing ratios closer to observations, but are not silver bullets.
- GEOS-Chem has seen significant changes in reactive nitrogen between 11-02 and 13.1.1. Our immediate next step will be to confirm whether this change is primarily in chemistry or in emissions.

This work has been funded by the University of Rochester and NASA. This work uses chemical transport model GEOS-Chem and data from the NASA Atmospheric Tomography mission.